Method of modelling the compaction behaviour of cylindrical pharmaceutical tablets

Norhayati Ahmat[*], Hassan Ugail[1], Gabriela González Castro[2]

Centre for Visual Computing, University of Bradford, Bradford BD7 1DP, UK

ABSTRACT

The mechanisms involved for compaction of pharmaceutical powders have become a crucial step in the development cycle for robust tablet design with required properties. Compressibility of pharmaceutical materials is measured by a force–displacement relationship which is commonly analysed using a well known method, the Heckel model. This model requires the true density and compacted powder mass value to determine the powder mean yield pressure. In this paper, we present a technique for shape modelling of pharmaceutical tablets based on the use of partial differential equations (PDEs). This work also presents an extended formulation of the PDE method to a higher dimensional space by increasing the number of parameters responsible for describing the surface in order to generate a solid tablet. Furthermore, the volume and the surface area of the parametric cylindrical tablet have been estimated numerically. Finally, the solution of the axisymmetric boundary value problem for a finite cylinder subject to a uniform axial load has been utilised in order to model the displacement components of a compressed PDE-based representation of a tablet. The Heckel plot obtained from the developed model shows that the model is capable of predicting the compaction behaviour of pharmaceutical materials since it fits the experimental data accurately.

© 2010 Elsevier B.V. All rights reserved.

1. Introduction

Tablets are the most popular dosage form for drug delivery in the pharmaceutical industry, occupying two thirds of the global market (Wu and Seville, 2009). This type of dosage form is convenient to use by patients, have long term storage stability and have good tolerance to changes in temperature and humidity. Additionally, they can be designed to protect unstable medications or disguise unpalatable ingredients. Tablets have been made in virtually any shape; most of them are round, oval or capsule shaped. The quality of the tablet is described by several parameters such as hardness, accurate mass, content uniformity and height (Belic et al., 2009).

Pharmaceutical tablets comprise a mixture of powder form components where all of them contribute to the final properties of the product. The tabletting process can be divided into three stages (Wu et al., 2008). First, the powder is filled into the die cavity. Secondly, a compaction process takes place which involves compression and decompression of the powder bed. Finally, the compacted powder is ejected from the die in the form of a tablet

after the required height is obtained. The tablets have to be strong enough to sustain any possible load after the compaction process such as film coating, packing and handling (Wu et al., 2005). It is agreed by Coube et al. (2005) that the properties of the tablet such as mechanical strength or disintegration depend significantly upon the powder behaviour during all three stages of the process. Therefore, it is very important to understand the mechanical behaviour of the powder during each stage for successful formulation processing.

In order to produce quality tablets, many studies have been carried out to investigate the compaction properties (compressibility and compactibility) of different types of excipients such as microcrystalline cellulose (Zhang et al., 2003; Hassanpour and Ghadiri, 2004) and lactose (Zhang et al., 2003; Hassanpour and Ghadiri, 2004; Ilić et al., 2009). Compressibility refers to the ability of the powder to change in volume when subjected to pressure (Ilić et al., 2009) whereas compactibility is the ability of powders to convert from small particles into coherent solid dosage form (Yap et al., 2008). The Heckel (Zhang et al., 2003; Hassanpour and Ghadiri, 2004; Ilić et al., 2009), Kawakita (Zhang et al., 2003) and modified Walker (Ilić et al., 2009) models are widely used approaches in studying the compressibility of pharmaceutical powders.

In this work, the practical and theoretical results of a compressed powder are analysed using the Heckel model. This model is developed by assuming that powder compression follows a first-order chemical reaction, where the pores are the reactant (Zhang

* Corresponding author. Tel.: +44 7507262565.
  E-mail addresses: n.b.ahmat@bradford.ac.uk (N. Ahmat), h.ugail@bradford.ac.uk (H. Ugail), g.gonzalezcastro1@bradford.ac.uk (G.G. Castro).
  [1] Tel.: +44 1274235464.
  [2] Tel.: +44 1274233993.

et al., 2003) and based on the force–displacement data which is converted to a relative density–pressure relationship (Heckel, 1961):

$$\ln\left(\frac{1}{1-\rho_{\text{rel}}}\right) = PK + A, \tag{1}$$

where ρ_{rel} is the relative density, P is the pressure, and K and A are constants. The relative density is the bulk density proportional to the true density

$$\rho_{\text{rel}} = \frac{\rho_{\text{bulk}}}{\rho_{\text{true}}}, \tag{2}$$

and $1 - \rho_{\text{rel}}$ represents the porosity. The slope, K and y-intercept, A of a linear graph are obtained when plotting the value of $\ln(1/(1-\rho_{\text{rel}}))$ against the applied axial pressure, P. The constant K gives the value of the plasticity of a compressed powder while A is associated with the particle rearrangement before deformation (Zhang et al., 2003). The reciprocal of K is a measure of the yield pressure, P_y of the particles that gives the value of the hardness of powders (Hassanpour and Ghadiri, 2004). Low values of P_y usually indicate harder tablets (Nokhodchi, 2005).

The Heckel model is suitable for materials that strengthen by plastic deformation (Yap et al., 2008) and works reasonably well for metal powders (Hassanpour and Ghadiri, 2004). Plastic deformation refers to the reduction in bulk volume of the powder bed when the applied external load has been removed from the bed (Owolabi et al., 2010). However, it has been reported that the Heckel analysis also has some drawbacks. The Heckel's parameter is very sensitive to small errors associated with experimental conditions (maximum pressure, punch displacements measurements and weight of the compact) and variations in the true density measurement (Hassanpour and Ghadiri, 2004; Ilić et al., 2009). Furthermore, the Heckel plot can be influenced by the particle size (Hassanpour and Ghadiri, 2004), the die size, the degree of lubrication and the overall time of compression (Sovány et al., 2009). Therefore, the effects of these variables should be taken into consideration when designing tablet formulations. However, the present work does not consider the last two factors when performing the compression process in order to obtain the experimental data. These factors will be taken into account in future work.

Compactibility can be estimated by measuring the mechanical strength of the pharmaceutical compact (Sonnergaard, 2006). The mechanical strength of cylindrical tablets can be characterised by the measurement of tensile strength (Wu and Seville, 2009). Tensile strength is a measure of the ability of a given material to resist forces that tend to pull it apart. This can generally be determined using the diametrical compression test (also known as Brazilian disk test), where the tablet is placed between two platens and compressed diametrically until it breaks or crushes. This test has been applied to both single component tablets and matrix tablets made of various components (Wu and Seville, 2009). Many studies have been carried out to explore the dependence of tensile strength on the properties of constituent components such as tablets' porosity, particle size and shape, and effective contact surface area.

The surface area and volume of tablets are two important features in characterising pharmaceutical compaction properties. It has been shown in Elkhider et al. (2007) that the density variation may affect the compact properties. Additionally, the work in Adolfsson et al. (1999) has proved that the surface area of a tablet influences the bonding mechanism of materials in the tablet. They have measured the hardness of a tablet by adjusting the tablet's surface area and the average distance between particles in compacts of different materials. They found that the adjustment gave similar bonding strength values for materials bonding mainly by weak distance forces.

Recently, the use of computer vision has been applied widely in medical applications especially in medical image processing (Peiró et al., 2007), designing drugs (Song et al., 2009), pharmaceutical tablet formulations (Yu et al., 2009) and simulation on various tablet processing techniques (Cunningham et al., 2004; Fu et al., 2006; Siiriä and Yliruusi, 2007). A number of methods have been proposed to simulate powder compression such as finite element (FE) (Wu et al., 2008) and discrete element (DE) (Hassanpour and Ghadiri, 2004) methods. However, it has been reported in Frenning (2008) that the implementation of the FE method is quite complicated and cannot distribute information on the particle range. Meanwhile, DE method fails to give an accurate result if the particle deformation is extensive and it is hard to obtain stresses within individual particles (Frenning, 2008). Thus, a combined FE/DE method has been introduced to overcome these problems (Frenning, 2010). However, we have not found any report in the literature regarding any work related to geometric modelling of pharmaceutical tablets either interactively or based on the use of parametric surface representation. Therefore, the objective of this paper is to model a solid flat-faced cylindrical pharmaceutical tablet interactively and to study the displacements on the compressed parametric-tablet by utilising the analytical solution of the Love's stress function subject to an appropriate set of boundary conditions. We aim to develop a mathematical model for pharmaceutical use in minimising the cost and time used during the powder compaction process.

At present, there exists a variety of methods that can be utilised to generate the geometry of pharmaceutical tablets such as Non-uniform rational B-Splines (NURBS) (Sánchez et al., 2004), Bézier surfaces (Shang et al., 2008), B-Spline (Pungotra et al., 2008) and also a surface representation technique based on the use of partial differential equations (PDEs) known as the PDE method (Ugail and Wilson, 2005). Among all these methods, the PDE method is the most suitable method for representing any given shape of a tablet and its components since it can generate surfaces of complex geometries from a small amount of parameters. The PDE method has been introduced in Computer-aided Design (CAD) as a solution of a particular type of elliptic PDEs to generate smooth parametric surfaces (Ugail, 2006). The shape of the surfaces generated by this method is based on a boundary representation and can easily be modified since it is characterised by data distributed around their boundaries.

Numerous studies have been carried out to exploit the full potential of the PDE methodology in visual computing fields, as well as studies of compatibility between surfaces generated by the PDE method and spline-based techniques (Monterde and Ugail, 2006). PDE surfaces offer many advantages over other type of surfaces. Most of all, they are a natural representation and offer a close representation to the real world because they are controlled by physical laws and can integrate geometric attributes with functional constraints for surface modelling, design and analysis. Furthermore, PDE surfaces can be easily associated with the physical world. For example, the parameters in the PDE can give a physical meaning such as elasticity and stiffness if they are formulated properly (Zhang and You, 2004). Moreover, smooth surfaces with high-order continuity requirements can be defined through PDEs since the formulation is well-conditioned and technically sound. This technique is also capable of blending surfaces (González Castro et al., 2008) and offers modelling tools to manipulate the shape of a PDE surface by altering the values of its design parameters (Ugail, 2006). Thus, a PDE-based model remains continuous when the values of its design parameters are changed. In the present context, this means that PDE surfaces can adapt to physical changes of the tablet when the tablet has been compressed axially or diametrically.

The rest of this paper is organised as follows. Section 2 describes the mathematical theory associated with the PDE method and the solution to its standard formulation. It also explains the methodology used to generate a parametric solid cylindrical tablet.

Section 3 contains the solution to an axisymmetric boundary value problem for a cylinder with assigned stresses previously used for compressing cylindrical objects together with details on the axial compression process used to characterise the displacement behaviour of pharmaceutical powders and the PDE-based surface representation tablet. Section 4 presents results for an axially compressed PDE-based tablet and finally, Section 5 presents the conclusions of this work.

2. The PDE method

The PDE method was initially introduced into the area of blend shape generation in CAD by Bloor and Wilson (1989). In recent years, PDE-based shapes have broadened their uses in shape description especially in graphics and modelling, design analysis and optimisation (González Castro et al., 2008).

The PDE method produces a parametric surface based on the use of elliptic PDEs, defined by two parameters u and v in a finite region $\Omega \subset R^2$ where $0 \leq u \leq 1$ and $0 \leq v \leq 2\pi$. The general form of an elliptic PDE over a two-dimensional parametric domain is given by

$$\left(\frac{\partial^2}{\partial u^2} + \alpha^2 \frac{\partial^2}{\partial v^2} \right)^{2r} \underline{\chi}(u, v) = 0, \tag{3}$$

where $\underline{\chi}(u, v)$ is the function defining a surface in 3D space in a domain Ω while α is an intrinsic parameter controlling the relative smoothness of the surface in the u direction and r defines the order of the PDE, and they are restricted to $\alpha \geq 1$ and $r \geq 1$ (Ugail, 2006). Note that, Eq. (3) is biharmonic if α and r are set to be 1. The full three-dimensional representation of $\underline{\chi}(u, v)$ can be written of the form

$$\underline{\chi}(u, v) = (\underline{\chi}_x(u, v), \underline{\chi}_y(u, v), \underline{\chi}_z(u, v)), \tag{4}$$

where it maps a point in (u, v) in Ω to a point in 3D space such that $R^2(\Omega) \rightarrow E^3$.

Elliptic PDEs similar to that shown in Eq. (3) can be solved by using different methods such as Separation of Variables, Integral Transform and FE Method. For this work, the approach undertaken is based on the approximate solution of Eq. (3). The PDE method generates a smooth surface patch by solving Eq. (3) subject to a set of periodic boundary conditions that are imposed at the edge of the surface. By taking $r = 1$, Eq. (3) transforms to the general form of a fourth-order Elliptic PDE and is solved analytically based on a set of 4 boundary conditions which relate how $\underline{\chi}(u, v)$ and its normal derivatives, $\partial \underline{\chi} / \partial u$ vary along $\partial \Omega$

$$\underline{\chi}(0, v) = \underline{P}_0(v), \tag{5}$$

$$\underline{\chi}(1, v) = \underline{P}_1(v), \tag{6}$$

$$\frac{\partial \underline{\chi}}{\partial u}(0, v) = \underline{d}_0(v), \tag{7}$$

$$\frac{\partial \underline{\chi}}{\partial u}(1, v) = \underline{d}_1(v). \tag{8}$$

$\underline{P}_0(v)$ and $\underline{P}_1(v)$ determine the position at the edges of the surface patch at $u = 0$ and $u = 1$ while $\underline{d}_0(v)$ and $\underline{d}_1(v)$ define the values of the normal derivatives at the respective boundary of the surface. The derivative conditions play an important role in determining the overall shape of the surface (Ugail, 2006). They are defined by the derivative vector along the boundary curves, where the magnitude and the direction of the derivative vector are determined by the difference between each point on the derivative curve and an associated point on the boundary curve. The shape of the surface can be manipulated interactively by changing the size and direction of the derivative vector.

The solution to Eq. (3) is thus found using the separation of variables method and can be written as

$$\underline{\chi}(u, v) = \underline{A}_0 + \sum_{n=1}^{\infty} [\underline{A}_n(u) \cos(nv) + \underline{B}_n(u) \sin(nv)], \tag{9}$$

where

$$\underline{A}_0 = \sum_{m=1}^{4} \underline{\alpha}_{0m} u^{m-1}, \tag{10}$$

$$\underline{A}_n = (\underline{a}_{n1} + \underline{a}_{n3} u)e^{\alpha nu} + (\underline{a}_{n2} + \underline{a}_{n4} u)e^{-\alpha nu}, \tag{11}$$

$$\underline{B}_n = (\underline{b}_{n1} + \underline{b}_{n3} u)e^{\alpha nu} + (\underline{b}_{n2} + \underline{b}_{n4} u)e^{-\alpha nu}. \tag{12}$$

The term $\underline{A}_0$ is a cubic polynomial on the parameter u tracing the spine of the surface patch that brings out the symmetries of that patch, $\sum_{n=1}^{\infty} [\underline{A}_n(u) \cos(nv) + \underline{B}_n(u) \sin(nv)]$ describes the radial position of the point $\underline{\chi}(u, v)$ away from a point at $\underline{A}_0(u)$, and $\underline{a}_{n1}$, $\underline{a}_{n2}$, $\underline{a}_{n3}$, $\underline{a}_{n4}$, $\underline{b}_{n1}$, $\underline{b}_{n2}$, $\underline{b}_{n3}$ and $\underline{b}_{n4}$ are vector-valued constants which values are determined by the imposed boundary conditions at $u = 0$ and $u = 1$ (Ugail, 2006). In order to define the different constants in the solution for a general set of boundary conditions, it is necessary to express the boundary conditions as Fourier series so that the corresponding coefficients are identified.

Since Eq. (9) gives infinite solutions, hence we need to find the approximation to this series. This is based on the sum of the first Fourier modes (typically $N = 6$) and a remainder function, $\underline{R}(u, v)$ which represents an error term since N is a finite value

$$\underline{\chi}(u, v) \cong \underline{F}(u, v) + \underline{R}(u, v), \tag{13}$$

where

$$\underline{F}(u, v) = \sum_{m=1}^{4} \underline{a}_{0m} u^{m-1} + \sum_{n=1}^{N} [\underline{A}_n(u) \cos(nv) + \underline{B}_n(u) \sin(nv)], \tag{14}$$

and

$$\underline{R}(u, v) = (\underline{r}_1(v) + \underline{r}_3(v)u)e^{\beta u} + (\underline{r}_2(v) + \underline{r}_4(v)u)e^{-\beta u}, \tag{15}$$

where $\beta = N(\alpha + 1)_4$ and $\underline{r}_1$, $\underline{r}_2$, $\underline{r}_3$ and $\underline{r}$ are obtained by considering the difference between the original boundary conditions and the boundary conditions satisfied by Eq. (14). Fig. 1 presents the effect of the derivative conditions $\partial \chi / \partial u$ on the shape of the surface where all the PDE surfaces have the same boundary conditions on the function χ whereas the boundary conditions on the function $\partial \chi / \partial u$ at $u = 0$ and $u = 1$ have been varied. Note that the derivative boundary conditions are found by comparing two auxiliary inner curves, with the boundary curves already associated with position accordingly. The boundary conditions have to be defined appropriately in order to create any freeform surface patch using the PDE method. The adjacent surface patch is created by evaluating the boundary conditions using the next set of curves. For the adjacent patch, one surface or part of it needs to be blended to another surface as shown in Figs. 2 and 3.

2.1. Modelling a parametric cylindrical pharmaceutical tablet

This section discusses how to use the PDE method for designing a generic pharmaceutical tablet shape. The geometric model representing a flat-faced cylindrical tablet used throughout this work has been obtained using 10 generating curves to produce a surface composed of 3 patches, since each surface patch requires 4 curves. Each curve is comprised by several points from 0 to 2π and the last point ensures that each curve is closed properly. Each of these curves represents a circle of a given radius at a particular height.

In order to use the PDE method to design a closed cylinder, the whole design procedure is split into several steps. First, the
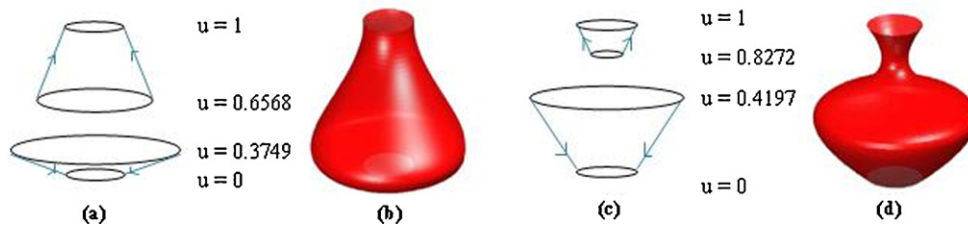
Fig. 1. Example of PDE surfaces generated by the PDE method. The boundary conditions defined in the form of curves in E^3 with different derivative conditions in (a) and (c). The resulting surface shape for each boundary conditions in (b) and (d).
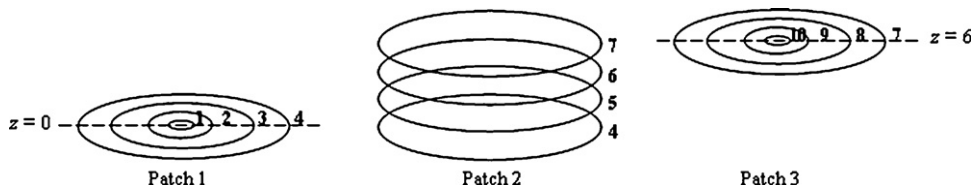

Fig. 2. The generating curves for a closed cylinder.

base of the cylinder (Patch 1) is generated followed by the body of that cylinder (Patch 2) and finally the top surface (Patch 3) is designed. Each patch share one boundary curve with either one or two different PDEs so that position continuity is guaranteed along the generated surface. As one can see in Fig. 2, the last curve of Patch 1 is used as the first curve of Patch 2 in order to ensure continuity between patches.

After creating all the necessary curves, the resulting surface for each patch is generated using the PDE method with the assigned boundary conditions. Therefore, 3 different PDEs have been solved using 5 Fourier modes. The output shape of the generated closed cylinder with radius 5 mm and height 6 mm is shown in Fig. 3(b) where all sets of curves in Fig. 3(a) are contained in the resulting surfaces. Note that the shape of each surface patch can easily be controlled by the shape of their boundary curves. Fig. 3(c) represents the resulting PDE surface with a restricted domain equivalent to $0 \leq u \leq 1$ and $(\pi/2) \leq v \leq 2\pi$.

2.2. Surface area and volume of a parametric cylindrical tablet

As mentioned in Section 1, the surface area and volume of pharmaceutical tablets play an important role in characterising compaction properties. Thus, it is necessary to measure the surface area and volume of PDE surfaces. The remaining part of this section shows formulae used to calculate both area and volume of parametric surfaces.

Eq. (4) has a vectorial representation of the form

$$\underline{\chi}(u, v) = \chi_x(u, v)\mathbf{i} + \chi_y(u, v)\mathbf{j} + \chi_z(u, v)\mathbf{k}, \tag{16}$$

where $\mathbf{i}$, $\mathbf{j}$ and $\mathbf{k}$ are the Cartesian basis vectors also known as unit vectors along x-, y- and z-axis respectively while χ_x, χ_y and χ_z rep-

resent the (x, y, z) coordinates of a given point in the surface. Since the shape of the generated tablet is a cylinder, there is no difference between the original boundary conditions of a cylinder and the boundary condition satisfied by the approximate solution of the elliptic PDE. Thus, R_x, R_y and R_z are all equal to zero and χ_x, χ_y and χ_z can be written as

$$\chi_x = A_{0x} + \sum_{n=1}^{N} [A_{nx} \cos(nv) + B_{nx} \sin(nv)], \tag{17}$$

$$\chi_y = A_{0y} + \sum_{n=1}^{N} [A_{ny} \cos(nv) + B_{ny} \sin(nv)], \tag{18}$$

$$\chi_z = A_{0z} + \sum_{n=1}^{N} [A_{nz} \cos(nv) + B_{nz} \sin(nv)]. \tag{19}$$

The surface area of $\underline{\chi}(u, v)$ is determined by

$$A(S) = \iint_{\Omega} \left| \frac{\partial \underline{\chi}}{\partial u} \times \frac{\partial \underline{\chi}}{\partial v} \right| d\Omega, \tag{20}$$

and the volume can be found by using

$$V(E) = \frac{1}{3} \iint_{\Omega} \underline{\chi} \left(\frac{\partial \underline{\chi}}{\partial u} \times \frac{\partial \underline{\chi}}{\partial v} \right) d\Omega, \tag{21}$$

where

$$\frac{\partial \underline{\chi}}{\partial u} = \frac{\partial \chi_x}{\partial u} \mathbf{i} + \frac{\partial \chi_y}{\partial u} \mathbf{j} + \frac{\partial \chi_z}{\partial u} \mathbf{k} \tag{22}$$

$$\frac{\partial \underline{\chi}}{\partial v} = \frac{\partial \chi_x}{\partial v} \mathbf{i} + \frac{\partial \chi_y}{\partial v} \mathbf{j} + \frac{\partial \chi_z}{\partial u} \mathbf{k}. \tag{23}$$
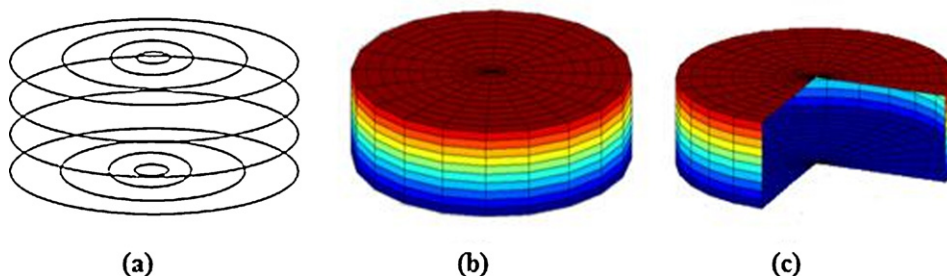

Fig. 3. Geometric model of a cylindrical tablet. Generated curves of a closed cylinder in (a). Resulting surface of a closed cylinder in (b) and (c).
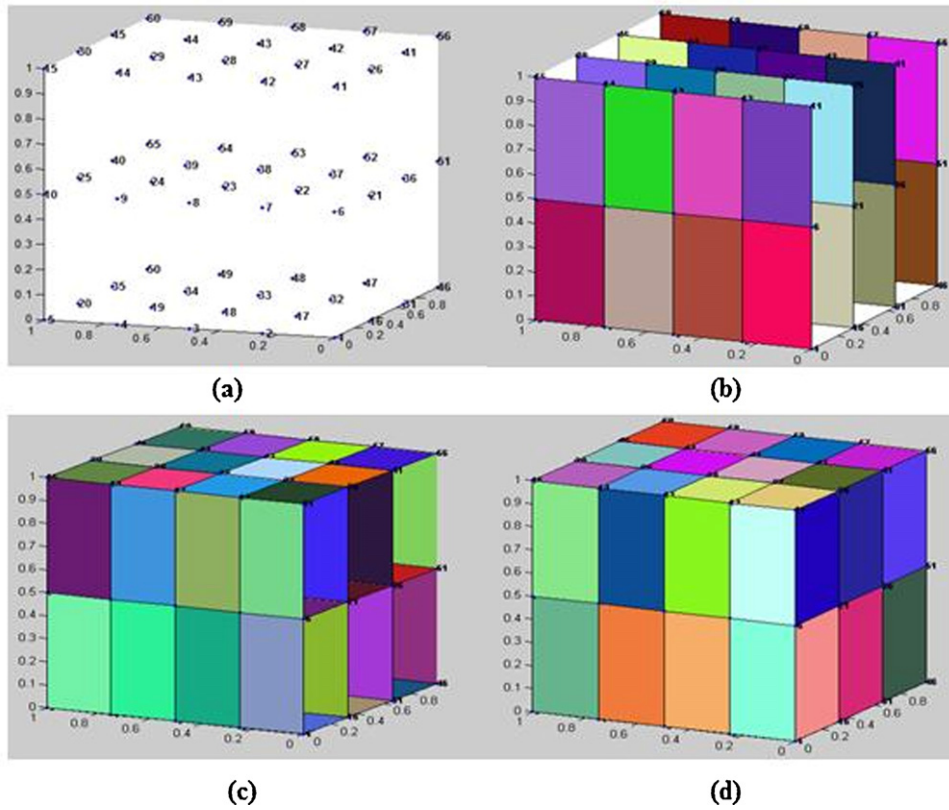
Fig. 4. Cuboid mesh generation process. Generated nodes in (a); generating Face1 faces parallel to *yz*-plane from front layer to *su*-layer in (b); generating Face2 faces parallel to *xy*-plane from bottom layer to *sw*-layer in (c); generating Face3 faces parallel to *zx*-plane from right layer to *sv*-layer in (d).

The total surface area and the volume of the generated parametric cylindrical tablet can be calculated numerically using MATLAB. The measured surface area and volume of each patch is given in Table 1, as well as the value of total surface area and volume obtained from the standard formulae $S = 2\pi r(r + h)$ and $V = \pi r^2 h$ respectively where $r = 5$ mm and $h = 6$ mm. Notice that the volume of Patch 3 is different from that of Patch 1. This is because Eq. (21) satisfies the Divergence Theorem of a closed surface whereby the unit normal vector **n** of Patch 1 points downwards and the **n** of Patch 3 is pointing upwards.

The total values of the tablet's surface area and volume calculated using Eqs. (20) and (21) are slightly different from values obtained from the standard formulae for obtaining the surface area and volume of a cylinder with height, h and radius, r. This difference attributed to the fact that both surface area and volume associated with the PDE-based model are obtained by solving the integrals numerically.

2.3. Simple three-dimensional mesh generation using the PDE method

In this section we discuss how to use the PDE method for generating a cuboid mesh for a cylindrical tablet. This cuboid mesh will

Table 1
The surface area and volume of each patch.

Patch	Surface area (mm^2)	Volume (mm^3)
1	78.361	0
2	188.340	313.597
3	78.361	156.723
Total	345.062	470.320
Formula	345.575	471.239

represent the inner part of the tablet since the PDE method's formulation used in Section 2.1 only generates the tablet's shell. The mesh generation algorithm is based on a simple mechanical analogy between a cuboid mesh and the boundary coefficients. Eq. (9) has been extended to a higher dimensional space by introducing a new parameter, w

$$\underline{\chi}(u, v, w) = \underline{A}_0(u) + w \sum_{n=1}^{\infty} [\underline{A}_n(u)\cos(nv) + \underline{B}_n(u)\sin(nv)], \qquad (24)$$

where $0 \le w \le 1$. As mentioned before, u and v define the parametric region while $\underline{A}_0$ and $\sum_{n=1}^{\infty}[\underline{A}_n(u)\cos(nv) + \underline{B}_n(u)\sin(nv)]$ describe the spine and distance of the $\underline{\chi}(u, v)$ to the spine of the surface patch respectively. This new parameter generates points for the interior of the object, from the spine towards the point $\underline{\chi}(u, v)$ on the surface.

Fig. 4 shows the outline of the cuboid mesh generation process. The number of nodes and cuboids used to generate the solid object depend on parameters u, v and w. For example in Fig. 4, parameters are defined as $u = [0, 0.333, 0.667, 1]$, $v = [0, 0.25, 0.5, 0.75, 1]$, and $w = [0, 0.5, 1]$, hence 60 nodes ($su \times sv \times sw = 4 \times 5 \times 3$) and 24 cuboids ($3 \times 4 \times 2$) are used to generate the solid. Parameters su, sv and sw represent the number of nodes of u, v and w on x-, y- and z-axis respectively.

All 6 faces of the cuboid are grouped into 3 sets of opposite faces: Face1 (parallel to yz plane), Face2 (parallel to xy plane) and Face3 (parallel to zx plane). Each Face1, Face2 and Face3 of a cuboid is generated by connecting 4 vertices. For a smooth mesh generation, Face1, Face2 and Face3 of all cuboids are generated layer by layer starting from Face1's layers followed by Face2's layers and ending at Face3's layers. The cuboid mesh generation is completed when all nodes have been connected to its neighbouring nodes and several cuboids are linked into one polyhedron where
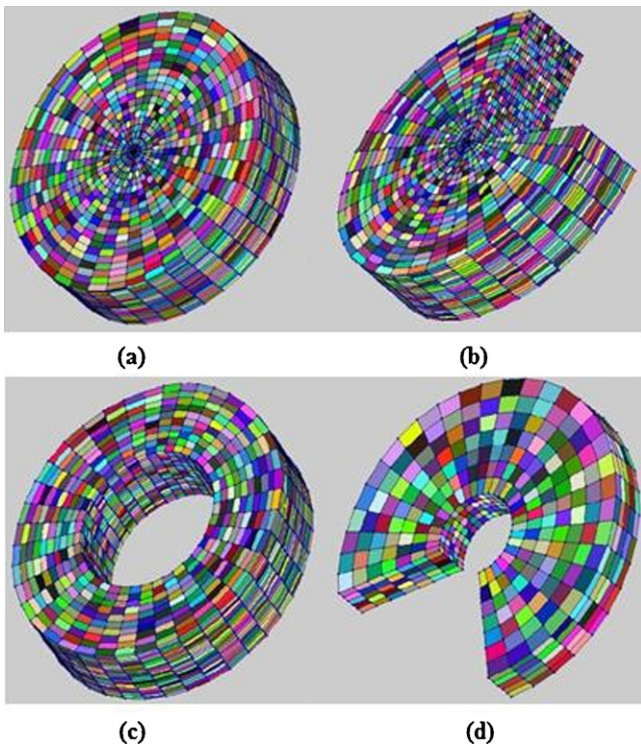
Fig. 5. Solid PDE-based representation of a cylindrical tablet. The complete tablet in (a). Examples of trimmed representations in (b)–(d).

its shape is defined by the boundary coefficients of the PDE surface.

The generated solid cylindrical tablet using the PDE method is shown in Fig. 5(a). This tablet is produced by defining both parameters u and w from 0 to 1 and they are divided into 20 equal parts respectively while the parameter v is delimited by $0, \pi/20, \pi/10, \ldots, 2\pi$, giving rise to 16,000 cuboids mesh. For many practical designs, sometimes a portion of the original surface needs to be removed. Thus, Ugail (2006) has proposed a method for trimming surfaces as solutions to PDEs and proved that the proposed method can be used to trim other types of parametric surfaces. Here, we show that a solid PDE-based representation of a tablet also can be trimmed by determining the new region of parameter space (u, v, w), where all the mesh points which do not belong to this region will be discarded. Fig. 5(b)–(d) shows some examples of cylindrical tablets. The tablet displays in Fig. 5(b) is obtained by choosing the parametric region to be $0 \leq u, w \leq 1$ and $(\pi/2) \leq v \leq 2\pi$. The number of cuboids in the cylindrical tablet in Fig. 5(c) is reduced to 8000 when the parameter w is set to be from 0.5 to 1. Fig. 5(d) represents a tablet when the region corresponding to $(0.5 \leq u \leq 1, \pi \leq v \leq (3/2)\pi, 0 \leq w \leq 0.3)$ has been trimmed out.

3. Axisymmetric stresses in a solid cylindrical object

A large number of practical problems involve geometrical features which have a natural axis of symmetry, such as a solid cylinder. For instance, the problem of equilibrium on an elastic cylinder of finite length subject to a surface load is one of the most discussed problems in the theory of elasticity (Sburlati, 2009). The use of a Love's stress function reduces the three-dimensional axisymmetric elastic problem into two-dimensional one.

Let us consider a circular, finite, homogeneous and isotropic elastic cylindrical object of thickness h and radius c, with the origin at the centre of the bottom plane subject to an axisymmetric load, q as illustrated in Fig. 6(a). The stress components acting on each face of the wedge from the loaded cylinder is visualised in Fig. 6(b). The normal stress components σ_z, σ_θ and σ_r are known respectively as the axial, hoop and radial stresses and are the principal stresses at a given stressed point, B. Each component has double subscripts (except for the normal stress components) where the first subscript defines the face on which the stress component acts and the second subscript denotes the direction in which the stress component acts. For instance, σ_z, τ_{zr} and $\tau_{z\theta}$ are stress components on the z surface and acting in the z, r and θ directions respectively. A stress component on a surface is considered positive if it acts parallel to direction of the corresponding axis.

The displacement of a solid cylinder due to external loads is completely described when the displacement of all its parts are defined respectively. In cylindrical coordinates, ω_z, ε_θ and μ_r are axial, hoop and radial displacements and parallel to the z, θ and r directions respectively. Any point originally at (z, θ, r) is displaced to $(z + \omega_z, \theta + \varepsilon_\theta, r + \mu_r)$ after the compression process is completed (Baxter-Brown, 1973). The components ε_θ, $\tau_{z\theta}$ and $\tau_{r\theta}$ vanish if the compression of the cylinder is due to torsionless axisymmetry.

In the case of the axisymmetric problem in the absence of body forces, the stress and displacement components can be expressed in terms of a Love's stress function $\phi(r,z)$ (Timoshenko and Goodier, 1970) as

$$\sigma_z = (2 - \gamma)\frac{\partial}{\partial z}\nabla^2\phi - \frac{\partial^3\phi}{\partial z^3}, \tag{25}$$

$$\sigma_r = \gamma\frac{\partial}{\partial z}\nabla^2\phi - \frac{\partial^3\phi}{\partial z\partial r^2}, \tag{26}$$

$$\tau_{rz} = (1 - \gamma)\frac{\partial}{\partial r}\nabla^2\phi - \frac{\partial^3\phi}{\partial r\partial z^2}, \tag{27}$$

$$\mu_r = -\frac{1}{2G}\frac{\partial^2\phi}{\partial z\partial r}, \tag{28}$$

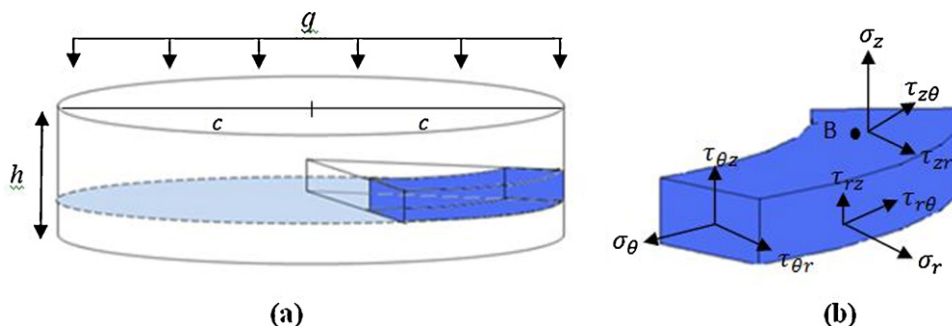$$\omega_z = \frac{1}{2G}\left[2(1 - \gamma)\nabla^2\phi - \frac{\partial^2\phi}{\partial z^2}\right], \tag{29}$$

Fig. 6. Stresses in cylindrical coordinates where σ_z, σ_θ and σ_r are the normal stress components in the z, θ and r directions respectively.
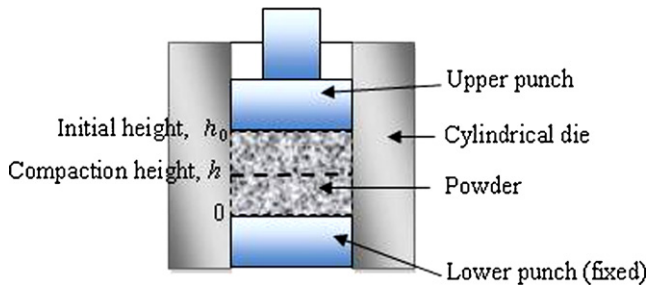
Fig. 7. An illustration of powder compaction process.

where G is the shear modulus and γ is the Poisson's ratio. The function $\phi(r,z)$ in Eqs. (25)–(29) is biharmonic and satisfies the following partial differential equation (Love, 1892):

$$\nabla^2\nabla^2\phi = \left(\frac{\partial^2}{\partial r^2} + \frac{1}{r}\frac{\partial}{\partial r} + \frac{1}{r^2}\frac{\partial^2}{\partial z^2}\right)^2 = 0, \tag{30}$$

where ∇^2 is the three-dimensional Laplace's operator.

A number of models have been developed and modified to find solutions of a symmetrically loaded cylinder that rigorously satisfies all the boundary conditions on the side surface or on both ends of the cylinder. One of them is the solution proposed by (Hao-Jiang et al., 2005). They found a three-dimensional analytical solution for a uniformly loaded isotropic circular plate by making use of the Love's stress function subject to two different types of clamped edges. The solution is obtained by utilising the biharmonic polynomial potential functions with 8 terms

$$\phi = \frac{1}{3}a_6(16z^6 - 120z^4r^2 + 90z^2r^4 - 5r^6) + b_6(8z^6 - 16z^4r^2$$
$$-21z^2r^4 + 3r^6) + a_4(8z^4 - 24z^2r^2 + 3r^4) + b_4(2z^4 + z^2r^2 - r^4)$$
$$+a_3(2z^3 - 3zr^2) + b_3(z^3 + zr^2) + a_2(2z^2 - r^2) + b_2(z^2 + r^2),$$
$$\tag{31}$$

where a_i, b_i ($i = 2,3,4,6$) are unknown constants to be determined from the boundary conditions. This work employed two different types of boundary conditions and the result showed that the different boundary conditions exert no influence on σ_z and τ_{rz} (Hao-Jiang et al., 2005).

In our work, Eq. (31) together with a particular set of boundary conditions will be used to measure the radial and axial displacements of an axially compressed PDE-based tablet. The results obtained from this model will be compared with the experimental results of the compressed pharmaceutical powder.

3.1. Experiment: axial compression on a pharmaceutical powder

Tablets of 3 mm in height were prepared at the Institute of Pharmaceutical Innovation (IPI), University of Bradford and were composed of 300 mg of α-lactose monohydrate (Pharmatose 200 M, DMV International, The Netherlands). Tablets were made by uniaxial compression using circular flat faced punches in a die with a diameter of 10 mm where the lower punch remains stationary as shown in Fig. 7. This process is known as Single Ended Compression (SEC) (Wu et al., 2008). The α-lactose monohydrate is a common excipient in a pharmaceutical tablet production. This is due to its stability, low hygroscopicity and hardness (Ilić et al., 2009), being capable of supporting external loads such a packaging but at the same time it has to be easy to dissolve so that it can be assimilated rapidly. Particle size for the powder was measured by Laser Diffractometer, Mastersizer 2000 Ver. 2.00 (Malvern Instruments, Malvern, UK) and the values range from 63 to 90 μm.
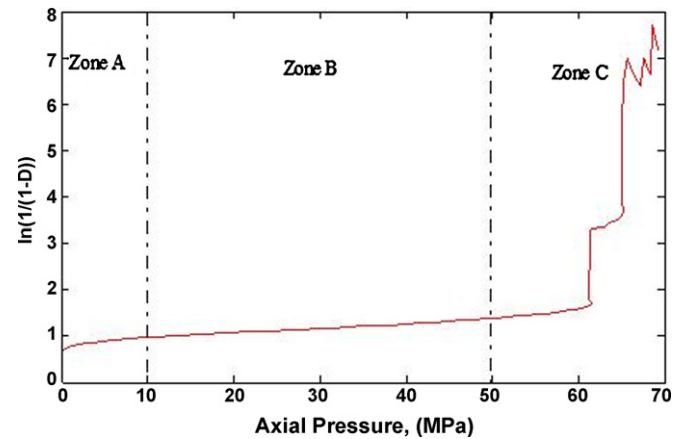

Fig. 8. The Heckel plot of the compressed α-lactose monohydrate using experimental data.

The α-lactose monohydrate with true density 1.3 mg/mm^3 was poured into a cylindrical die. The true density of the powder was measured using an Accupyc 1330 helium pycnometer (Micromeritics Ltd.). The density–pressure profile was obtained by using the "in-die" method where the compacts dimensions were measured from the punch displacements. The powder was compressed and decompressed by the upper punch at 100 mm/s. The values of the load and displacement were taken only after the load starts increasing and until it is linear. When the punch reaches the height of approximately 6 mm it starts receiving the resistance from the powder as it starts rearranging itself and the load starts increasing from 0.05 MPa. The load continues to increase linearly until a compact is formed and once the compact with maximum strength is formed the load and displacement relation is no longer linear. The powder compression process only involved an axial displacement, that is, the radius is fixed and only the height of the compressed powder is changed.

The experimental data (a set of force and displacement data) together with the fixed true density and compacted mass value were analysed using the Heckel model from which powder deformation mechanisms are determined using the apparent yield pressure. However, experimental data are commonly not linear as can be seen in Fig. 8. Some curves exist at very low pressure (Zone A) and high pressure (Zone C) regions and linearity is only showed in the centre pressure range (Zone B). The curvature at Zone A is due to particle rearrangement and fragmentation while it is agreed that the linear part represents particle plastic deformation (Gabaude et al., 1999). For the Heckel analysis, only data from pressure 10 MPa up to 50 MPa (Zone B) are used because this range showed the best linearity.

3.2. Simulation: axial compression on the PDE-based tablet

The radial and axial displacements in the PDE-based tablet can be obtained by substituting Eqs. (25) and (27)–(30) into a set of boundary conditions

$$\sigma_z = 0, \quad \tau_{rz} = 0 \text{ when } z = 0;$$

$$\sigma_z = -q, \quad \tau_{rz} = 0 \text{ when } z = h_0;$$

$$\omega_z = 0, \quad \frac{\partial \omega_z}{\partial r} = 0 \text{ when } z = 0;$$

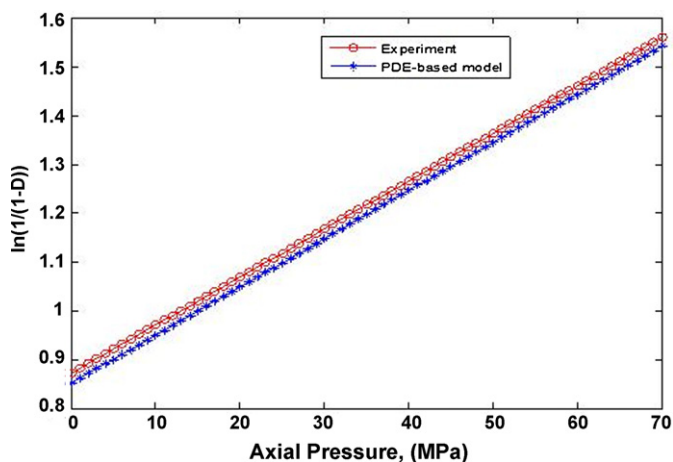$$\mu_r = 0 \quad \text{when } r = c. \tag{32}$$

Fig. 9. Comparison between the Heckel plot of the simulated compression and experiment on lactose powder.

Thus, Eqs. (28) and (29) can be written as

$$\mu_r = \frac{qz\gamma}{4Gh_0}\left(r - \frac{c^2}{r}\right), \quad r > 0 \tag{33}$$

$$\omega_z = \frac{qz^2}{2Gh_0}\left[\frac{z^2\gamma}{r^2} - \frac{1-\gamma}{2} + \frac{\gamma^2}{\gamma-1}\left(1 - \frac{c^2}{r^2}\right)\right], \quad r > 0 \tag{34}$$

where q is the axial force, c is the radius of the die or tablet, h_0 is the initial height of the powder bed or tablet, z and r are any point in z and r directions respectively while G is given by

$$G = \frac{E}{2(1+\gamma)}, \tag{35}$$

where E is the Young's modulus. The values of the Young's modulus and Poisson's ratio of α-lactose monohydrate are $E = [2.55, 4.35]$ GPa and $\gamma = [0.12, 0.5]$ respectively (Perkins et al., 2007).

4. Results and discussions

Due to the different initial porosity of the particles used in the experiment and simulation based on the PDE-based formulation proposed in this work, Eq. (34) has been modified by adding an adjustment constant, ω_{z0},

$$\omega_z = \omega_{z0} + \frac{qz^2}{2Gh_0}\left[\frac{z^2\gamma}{r^2} - \frac{1-\gamma}{2} + \frac{\gamma^2}{\gamma-1}\left(1 - \frac{c^2}{r^2}\right)\right], \tag{36}$$

This constant is obtained from the difference between the initial axial displacement (after the particle rearrangement – Zone A) of the experiment and the simulation (PDE-based model).

The density–pressure relationship for the lactose powder is plotted as a best linear regression line as shown in Fig. 9 and the trend is compared with the simulation prediction. The simulation is displayed graphically by using the value of $E = 2.64$ GPa, $\gamma = 0.21$ and $\omega_{z0} = -1.0778$. It is observed that the developed model does fit the data within an acceptable discrepancy since the slopes of the simulation and experimental data are quite similar. However, both lines have a slightly different y-intercept.

Table 2 summarises the estimated data obtained from the Heckel diagram for both simulation and experiment. For this study,

Table 2
Heckel's parameters for α-lactose from experiment and simulation.

Type of compression	Slope, K	y-Intercept, A
Experiment	0.0098	0.8738
PDE-based model	0.0099	0.8524

the calculated yield pressure is 102.04 MPa. The plasticity of this material is very low since it has a low value of K (or high yield pressure). Furthermore, the difference between the y-intercept of the experiment and simulation is too small, and this is expected because of the simulation's axial displacement values are calculated from the parametric pharmaceutical tablet.

The results shown in Table 2 and Fig. 9 prove that the solution of Love's stress function can be utilised to measure the displacement components of the compressed solid PDE-based tablet. However, the validity of the developed mathematical model is only verified at lower forces which represent the plastic deformation of the powder. Additionally, this model only can be applied to flat-faced cylindrical tablets produced through SEC process. Consequently, a more general model for characterising the stress distribution should be developed.

Additionally, it is worth noting that the example of the tablet used throughout this work may give the reader the impression that the shape of the tablet is somehow restricted to cylindrical shapes. This is not the case since different tablet's shape can easily be formed using the PDE method by changing the shape of the boundary curves.

5. Conclusions

The work presented in this paper focuses on the application of the PDE method for designing a parametric representation of a given pharmaceutical tablet. The volume and surface area of the generic cylindrical tablet can be determined by using the formula of parametric surface and the values can be obtained numerically using MATLAB software. The solid PDE-based tablet can be generated by introducing an additional parameter, w into the analytical solution of the elliptic PDE. This variable generates points from the centreline or spine of the patch towards its surface. Additionally, the generated solid tablet can be trimmed by changing the region defined by independent variables u, v or w.

The displacement components of a compressed PDE-based tablet can be measured by utilising one of the solutions of the Love's stress function found in literature to model compression of pharmaceutical powders. The result is plotted in Heckel diagram and it is found that the theoretical Heckel's parameter is similar to the practical ones. However, the model seems to underestimate the initial volume of the particle bed. This may be attributed to the lack of detailed information on powder behaviour at low pressure.

This study shows that the simulation can be used to represent the powder compaction process as well as predicting the elasticity and plasticity of pharmaceutical materials. Hence, this model is capable to satisfy the industrial requirement and encourages future development of pharmaceutical technologies through computer based simulations. It has highlighted that the validity of the developed model is only for the linear portion of the Heckel analysis of the compressed powder. Additionally, the output of this model is sensitive to the change of the elastic properties such as the Young's modulus and Poisson's ratio.

References

Adolfsson, Å.S., Gustafsson, C., Nyström, C., 1999. Use of tablet tensile strength adjusted for surface area and mean interparticulate distance to evaluate dom-

inating bonding mechanisms. Drug Development and Industrial Pharmacy 25, 753–764.

Baxter-Brown, J.M., 1973. Introductory Solid Mechanics. John Wiley & Sons, London.

Belic, A., Skrjanc, I., Bozic, D.Z., Karba, R., Vrecer, F., 2009. Minimisation of the capping tendency by tabletting process optimisation with the application of artificial neural networks and fuzzy models. European Journal of Pharmaceutics and Biopharmaceutics 73, 172–178.

Bloor, M.I.G., Wilson, M.J., 1989. Generating blend surfaces using partial differential equations. Computer-Aided Design 21, 165–171.

Coube, O., Cocks, A.C.F., Wu, C.Y., 2005. Experimental and numerical study of die filling, powder transfer and die compaction. Powder Metallurgy 48, 68–76.

Cunningham, J., Sinka, I., Zavaliangos, A., 2004. Analysis of tablet compaction. I. Characterization of mechanical behavior of powder and powder/tooling friction. Journal of Pharmaceutical Sciences 93, 2022–2039.

Elkhider, N., Chan, K.L.A., Kazarian, S.G., 2007. Effect of moisture and pressure on tablet compaction studied with FTIR spectroscopic imaging. Journal of Pharmaceutical Sciences 96, 351–360.

Frenning, G., 2008. An efficient finite/discrete element procedure for simulating compression of 3D particle assemblies. Computer Methods in Applied Mechanics and Engineering 197, 4266–4272.

Frenning, G., 2010. Compression mechanics of granule beds: a combined finite/discrete element study. Chemical Engineering Science 65, 2464–2471.

Fu, X., Dutt, M., Bentham, A.C., Hancock, B.C., Cameron, R.E., Elliott, J.A., 2006. Investigation of particle packing in model pharmaceutical powders using X-ray microtomography and discrete element method. Powder Technology 167, 134–140.

Gabaude, C.M.D., Guillot, M., Gautier, J.C., Saudemon, P., Chulia, D., 1999. Effects of true density, compacted mass, compression speed, and punch deformation on the mean yield pressure. Journal of Pharmaceutical Sciences 88, 725–730.

González Castro, G., Ugail, H., Willis, P., Palmer, I., 2008. A survey of partial differential equations in geometric design. The Visual Computer 24, 213–225.

Hao-Jiang, D., Xiang-Yu, L., Wei-Qiu, C., 2005. Analytic solutions for a uniformly loaded circular plate with clamped edges. Journal of Zhejiang University (Science) A 10, 1163–1168.

Hassanpour, A., Ghadiri, M., 2004. Distinct element analysis and experimental evaluation of the Heckel analysis of bulk powder compression. Powder Technology 141, 251–261.

Heckel, R.W., 1961. Density–pressure relationship in powder compaction. Transactions of the Metallurgical Society of AIME 221 (4), 671–675.

Ilić, I., Kása, P., Dreu, R., Pintye-Hódi, K., Srčič, S., 2009. The compressibility and compactibility of different types of lactose. Drug Development and Industrial Pharmacy 35, 1271–1280.

Love, A.E.H., 1892. A Treatise of the Mathematical Theory of Elasticity. Cambridge University Press, Cambridge.

Monterde, J., Ugail, H., 2006. A general 4th-order PDE method to generate Bezier surfaces from the boundary. Computer Aided Geometric Design 23, 208–225.

Nokhodchi, A., 2005. An overview of the effect of moisture on compaction and compression. Pharmaceutical Technology 29, 46–66.

Owolabi, B.I.O., Afolabi, T.A., Adebowale, K.O., 2010. Effect of heat moisture treatment on the functional and tabletting properties of corn starch. African Journal of Pharmacy and Pharmacology 4 (7), 498–510.

Peiró, J., Formaggia, L., Gazzola, M., Radaelli, A., Rigamonti, V., 2007. Shape reconstruction from medical images and quality mesh generation via implicit surfaces. International Journal for Numerical Methods in Fluids 53, 1339–1360.

Perkins, M., Ebbens, S.J., Hayes, S., Roberts, C.J., Madden, C.E., Luk, S.Y., Patel, N., 2007. Elastic modulus measurements from individual lactose particles using atomic force microscopy. International Journal of Pharmaceutics 332, 168–175.

Pungotra, H., Knopf, G.K., Canas, R., 2008. Efficient algorithm to detect collision between deformable B-spline surfaces for virtual sculpting. Computer-Aided Design 40, 1055–1066.

Sánchez, H., Moreno, A., Oyarzun, D., García-Alonso, A., 2004. Evaluation of NURBS surfaces: an overview based on runtime efficiency. Journal of WSCG 11, 1213–6972.

Sburlati, R., 2009. Three-dimensional analytical solution for an axisymmetric biharmonic problem. Journal of Elasticity 95, 79–97.

Shang, L., Jiachuan, S., Li, H., Fan, C., 2008. Simulation of 3D garment based on six pieces of Bezier curved surfaces. IEEE Transactions on Visualization and Computer Graphics, 1082–1085.

Siiriä, S., Yliruusi, J., 2007. Particle packing simulations based on Newtonian mechanics. Powder Technology 174, 82–92.

Song, C.M., Lim, S.J., Tong, J.C., 2009. Recent advances in computer-aided drug design. Briefings in Bioinformatics 10, 579–591.

Sonnergaard, J.M., 2006. Quantification of the compactibility of pharmaceutical powders. European Journal of Pharmaceutics and Biopharmaceutics 63, 270–277.

Sovány, T., Kása Jr., P., Pintye-Hódi, K., 2009. Comparison of the halving of tablets prepared with eccentric and rotary tablet presses. AAPS PharmSciTech 10, 430–436.

Timoshenko, S.P., Goodier, J.N., 1970. Theory of Elasticity, 3rd ed. McGraw Hill, New York.

Ugail, H., 2006. Method of trimming PDE surfaces. Computers & Graphics 30, 225–232.

Ugail, H., Wilson, M., 2005. Modelling of oedemous limbs and venous ulcers using partial differential equations. Theoretical Biology and Medical Modelling 2, 28.

Wu, C.Y., Best, S.M., Bentham, A.C., Hancock, B.C., Bonfield, W., 2005. A simple predictive model for the tensile strength of binary tablets. European Journal of Pharmaceutical Sciences 25, 331–336.

Wu, C.Y., Hancock, B.C., Mills, A., Bentham, A.C., Best, S.M., Elliott, J.A., 2008. Numerical and experimental investigation of capping mechanisms during pharmaceutical tablet compaction. Powder Technology 181, 121–129.

Wu, C.Y., Seville, J.P.K., 2009. A comparative study of compaction properties of binary and bilayer tablets. Powder Technology 189, 285–294.

Yap, S.F., Adams, M.J., Seville, J.P.K., Zhang, Z., 2008. Single and bulk compression of pharmaceutical excipients: evaluation of mechanical properties. Powder Technology 185, 1–10.

Yu, D.-G., Branford-White, C., Yang, Y.-C., Zhu, L.-M., Welbeck, E.W., Yang, X.-L., 2009. A novel fast disintegrating tablet fabricated by three-dimensional printing. Drug Development and Industrial Pharmacy 35, 1530–1536.

Zhang, J.J., You, L.H., 2004. Fast surface modelling using a 6th order PDE. Computer Graphics Forum 23, 311–320.

Zhang, Y., Law, Y., Chakrabarti, S., 2003. Physical properties and compact analysis of commonly used direct compression binders. AAPS PharmSciTech 4 (Article No. 62).